Magnetic phase diagram of ε^{′}-FeH

Jianjun Ying, Jiyong Zhao, Wenli Bi, E. Ercan Alp, Yuming Xiao, Paul Chow, Guoyin Shen, and Viktor V. Struzhkin

Phys. Rev. B **101**, 020405 — Published 14 January 2020

DOI: 10.1103/PhysRevB.101.020405

Unexpected complex magnetic phase diagram of ε'-FeH

Jianjun Ying,[1,2,*] Jiyong Zhao,[3] Wenli Bi,[3,4,5] E. Ercan Alp,[3] Yuming Xiao,[6] Paul Chow,[6] Guoyin Shen,[6] and Viktor V. Struzhkin[7,2,†]

[1]*Department of Physics, and CAS Key Laboratory of Strongly-coupled Quantum Matter Physics, University of Science and Technology of China, Hefei, Anhui 230026, China*
[2]*Geophysical Laboratory, Carnegie Institution of Washington, Washington, DC 20015, USA.*
[3]*Advanced Photon Source, Argonne National Laboratory, Argonne, Illinois 60439, United States*
[4]*Department of Geology, University of Illinois at Urbana-Champaign, Urbana, Illinois 61801, USA*
[5]*Department of Physics, University of Alabama at Birmingham, Birmingham, AL 35294, USA*
[6]*HPCAT, X-ray Science Division, Argonne National Laboratory, Argonne, IL 60439United States*
[7]*Center for High Pressure Science and Technology Advanced Research, Shanghai, P. R. of China.*

(Dated: January 6, 2020)

Iron hydrides attract significant interest as candidates for the main constituents of the Earth′s core in geophysics and planetary science. However, their basic physical properties are still not well known. Here, we combined high pressure transport, synchrotron radiation Mössbauer and Fe K_β x-ray emission spectroscopy measurements on ε'-FeH to map out the detailed magnetic phase diagram of this hydride phase of iron. In contrast to our original expectations, we found two magnetic phase transitions at high pressure due to two inequivalent iron sites existing in ε'-FeH structure. Our results account for the previous large pressure difference on the loss of ferromagnetism between experiment and theoretical calculations. The discovery of unexpected complex magnetic phase diagram in ε'-FeH has implications to better understanding of the magnetic and physical properties of the iron-hydrogen compounds, important for the conditions of planetary interiors.

PACS numbers:

It is believed that the core of our planet is mainly composed of iron-rich alloy with dissolution of one or more lighter elements[1–3]. Hydrogen has been proposed as a possible major light element in the earth core[4–6] because iron hydride (FeH_x) can be formed by the reaction between iron and water under high pressures, however, the exact composition is still uncertain. Thus, detailed investigation of iron hydrides would have significant implications for our understanding of the physics and chemistry of the earth's core.

The ferromagnetic α-iron(bcc structure) looses its magnetism under pressure around 13 GPa, concomitant with the structural transition to hcp structure (ε-iron)[7]. Meanwhile, superconductivity below 2 K was detected in the non-magnetic ε-iron phase[8]. The dhcp ε'-FeH can be synthesized from the reaction of Fe and fluid H_2 at high pressures above 3$\sim$4 GPa at ambient temperature[9]. Hydrogenation of iron modifies considerably its crystal structure, electric resistivity and magnetic properties[10,11]. The ε'-FeH phase exhibits ferromagnetic properties, in contrast to the nonmagnetic high pressure phase of ε-Fe. Previous room-temperature synchrotron Mössbauer spectroscopy suggests ε'-FeH would lose its ferromagnetism above 22$\sim$30GPa[12], which is much lower than the theoretical calculation[13]. However, low temperature experiments are still missing to tracing the superconductivity and mapping out the detailed magnetic phase diagram. The ε'-FeH is stable at least up to 80 GPa, and compression behavior shows anomaly at 30 to 50 GPa[14]. However, whether such anomalies are related to the changes in magnetic properties is still unknown. Thus, detailed investigation of magnetic properties of ε'-FeH might be crucial to understand its high pressure anomalies. Here, we combined the low-temperature transport, synchrotron Mössbauer and Fe K_β x-ray emission spectroscopy(XES) measurements to study in detail the magnetic properties of ε'-FeH. To our surprise, the magnetism did not completely disappear at low-temperatures as reported in previous ambient temperature results. The relative weights of ordered magnetic moments are decreasing sharply around 26 GPa and 43 GPa. These two anomalies are consistent with the structural anomaly observed in the previous work[14]. In addition, XES result also shows anomaly above 43 GPa, which indicates the change of iron's local magnetic properties in the course of the second magnetic phase transition. Our results indicate that the ε'-FeH exhibits much more complex magnetic phase diagram due to the presence of two inequivalent iron sites. These results may have further implication to the understanding the physical properties of this iron hydride in the planetary interiors.

ε'-FeH samples were prepared by directly loading hydrogen and Fe in the Diamond anvil cell. We conducted the electrical transport measurements under pressure by using the miniature diamond anvil cell[15]. Diamond anvil with 300 μm culet and c-BN gasket with sample chambers of diameter 90 μm were used for the transport measurement. The longitudinal and Hall resistance were measured using the Quantum Design PPMS-9 equipment. Synchrotron Mössbauer spectroscopy measurements were performed at 3-IDB at the Advanced Photon Source. A gas membrane-driven miniature panoramic diamond anvil cell and specially designed flow cryostat was used[16,17]. The spectra were fitted by using the CONUSS software[18]. Diamond anvils with 160 μm culet

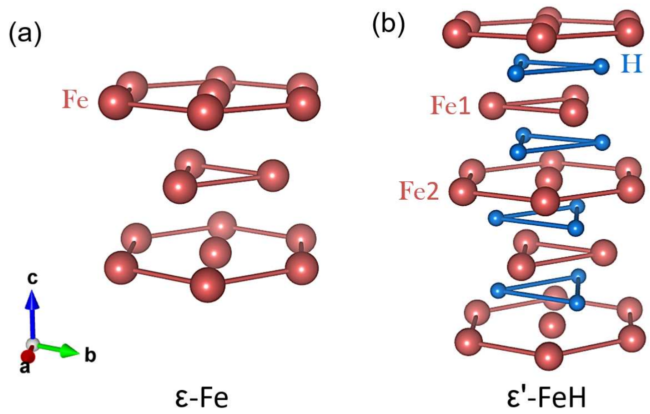

FIG. 1: (color online). The crystal structures of ε-iron (a) and ε'-FeH (b). The two crystallographically inequivalent iron sites are labeled as Fe1 and Fe2, respectively

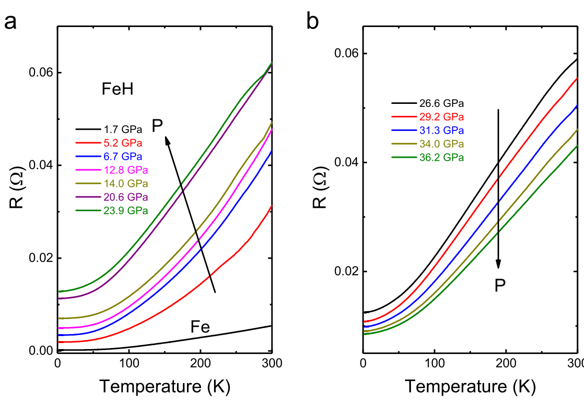

FIG. 2: (color online). The temperature dependence of the resistance for ε'-FeH under various pressures. (a) The resistance increases steeply after the reaction of iron with hydrogen above 4 GPa, and then it increases continuously with increasing pressure. (b) The resistance starts to decrease above 25 GPa, which is due to the magnetic transition. All the resistance curves show metallic behavior and no superconductivity is detected down to 2 K.

and Be gasket were used for the x-ray emission spectroscopy(XES) measurement. The room-temperature XES measurements were performed at 16-IDD of the High-Pressure Collaborative Access Team (HPCAT) at the Advanced Photon Source.

The ε'-FeH structure has ABAC stacking of Fe triangular layers with hydrogen occupying octahedral interstitial positions as shown in the Figure 1. In the ε'-FeH, there are two crystallographically inequivalent iron sites 2a(Fe2, (0, 0, 0)) and 2c(Fe1, (1/3, 2/3, 1/4)) in the Wyckoff representation. The two inequivalent iron sites would result in two magnetic six-line patterns in the Mössbauer experiment[19,20].

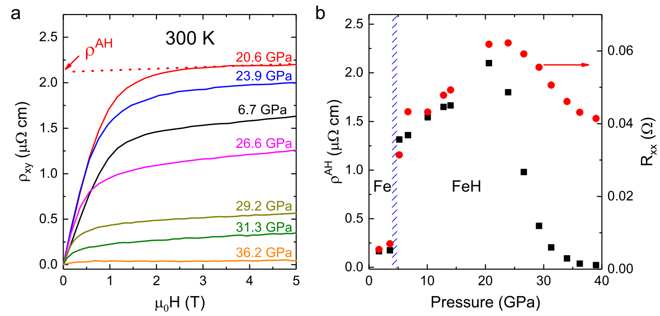

FIG. 3: (color online). (a) The anomalous Hall effect as measured at 300 K, which confirms the ferromagnetism in ε'-FeH. (b) The anomalous Hall resistivity ρ^{AH} rapidly decreases around 25 GPa, which is consistent with the loss of ferromagnetism found previously[12].

We performed the measurements of the temperature dependence of the resistance under various pressures as shown in the Figure 2. Below 4 GPa, the resistance of iron shows metallic behavior. At high pressure, iron would react with hydrogen and form ε'-FeH. The resistance increases after the reaction as previously reported in Ref.[11]. The resistance continuously increases with increasing pressure up to 25 GPa.The resistance starts gradually decrease above 25 GPa. The reduction of the resistance might be due to the sudden loss of the ferromagnetism in the ε'-FeH above 25 GPa. The resistance exhibits metallic behavior and no superconductivity was discovered down to 2 K at pressures up to 40 GPa.

We also performed the Hall measurements at 300 K under various pressures as shown in the Fig.3 (a). The giant anomalous Hall effect confirms the ferromagnetism in the ε'-FeH. We can obtain the anomalous Hall resistivity ρ^{AH} by extrapolating the linear Hall resistivity part at high magnetic field. The maximum value of the ρ^{AH} is about one order of magnitude larger than in pure iron. The anomalous ρ^{AH} rapidly decreases around 25 GPa, and resistance also starts to decrease above that pressure. These results are consistent with the loss of ferromagnetism at high pressures. However, ρ^{AH} does not reach zero above 25 GPa, which indicates that the magnetism is not completely suppressed at high pressure. This finding brings up more complicated magnetic phase diagram than previously thought.

In order to investigate the magnetic properties under high pressure, we performed low-temperature synchrotron Mössbauer measurement at high pressure. We show Mössbauer spectra under different pressures and temperatures in the Figure 4. The magnetic low pressure phase can be fitted by assuming two magnetic Fe sites accompanied with small portion of nonmagnetic Fe site(<5%), which may be related to the unreacted nonmagnetic hcp iron. At 300 K, the rapid oscillations related to the ordered magnetic moments suddenly disappear above 26 GPa, which is consistent with the previous

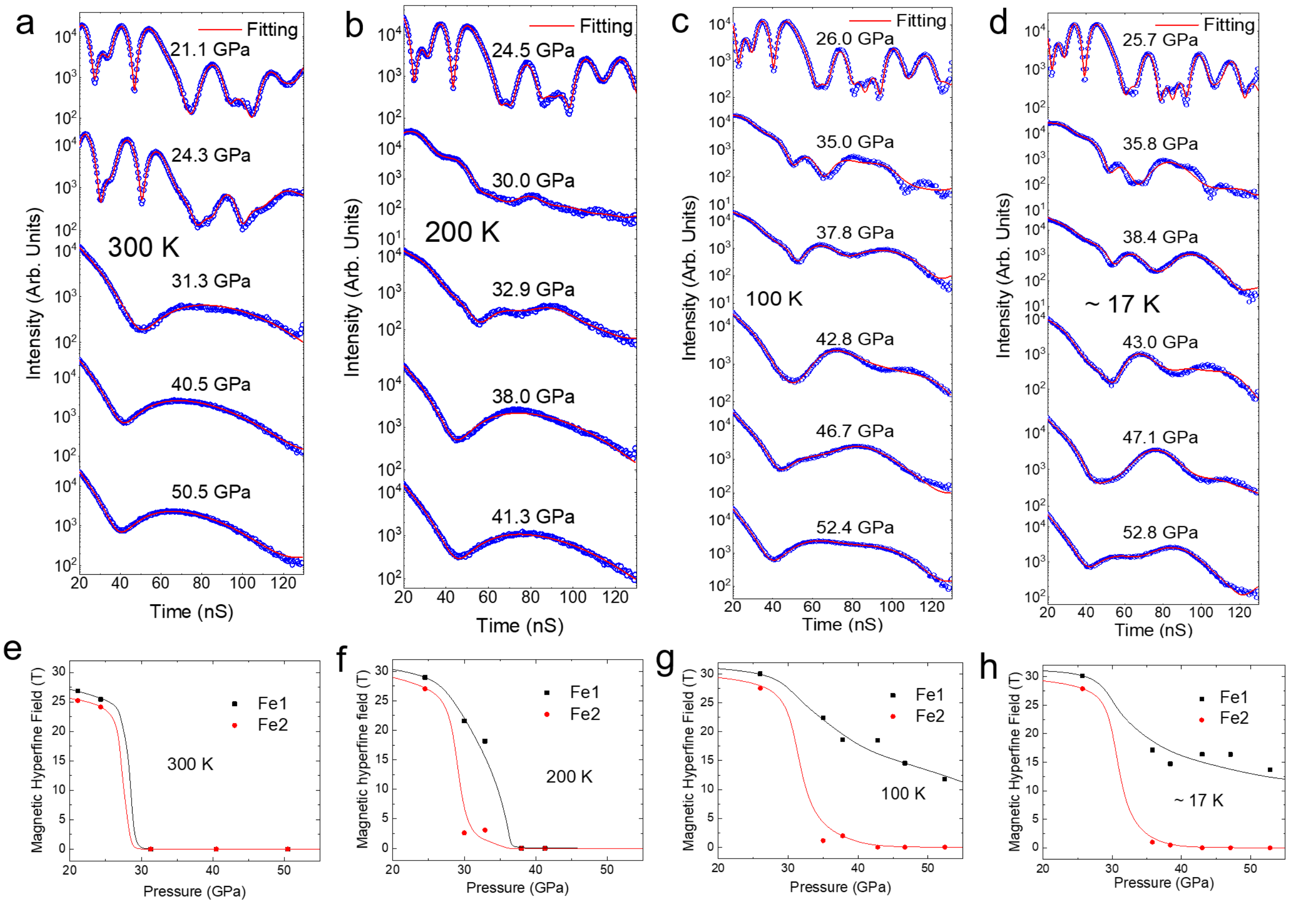

FIG. 4: (color online). (a)-(d) The high pressure synchrotron Mössbauer measurements of ε'-FeH under various temperatures. The red lines are the fits. (e)-(h) The hyperfine magnetic fields at the Fe1 and the Fe2 sites are obtained from the fits. At all temperatures, the hyperfine magnetic fields drop above 26 GPa, however, the value of the hyperfine field at the Fe1 site stays at 15$\sim$20 T below 200 K indicating the remaining magnetism at high pressure. The black and red lines are guide for the eye.

results[12]. However, with decreasing temperature, the oscillations persists to much higher pressures. The spectra at higher pressures can be fitted by invoking one or two magnetic Fe sites, and one nonmagnetic site. The two different magnetic Fe sites are due to the two inequivalent iron sites in the dhcp phase. We can obtain the magnetic hyperfine fields of both the two magnetic Fe sites from the fits. From previous Mössbauer results, the hyperfine field of the Fe1 site is slightly larger than on the Fe2 site[19,20], thus, we attribute the larger hyperfine field to the Fe1 site in all the fits. The hyperfine fields of both the Fe1 and Fe2 sites show sudden decrease at pressure above 26 GPa. These results are consistent with the loss of ferromagnetism above 26 GPa. However, the hyperfine field of the Fe1 site only drops to $\sim$20 T and gradually decreases with increasing pressure at low temperature. These results indicate that the Fe1 and the Fe2 sites show completely different magnetic phase diagrams although their original hyperfine fields are only slightly different.

We can also obtain the weight of ordered moments from the fitting results as shown in the Figure 5. The ordered magnetic part of the Fe1 and the Fe2 sites decreases to 30$\sim$40% above 26 GPa. Above 43 GPa, the weight of ordered moments shows another sudden decrease at low temperature. Above 43 GPa, a small portion of ordered moments is still left ($\sim$4%) at low temperature and is gradually suppressed with increasing pressure. We can conclude that the first sudden reduction of the ordered moments is mainly related to the loss of magnetism at the Fe2 site. The second sudden decrease above 43 GPa is related to the Fe1 site. In order to extract more information on magnetic properties of ε'-FeH under pressure, we performed high pressure Fe K_β XES measurements up to 1 Mbar to probe directly the total local spin properties related to the local magnetic moments. In order to quantitatively derive the total local moments pressure dependence from the K_β line, we used the integrated intensity of the difference spectra around the satellite peak as described in the supplemental material[21](see,

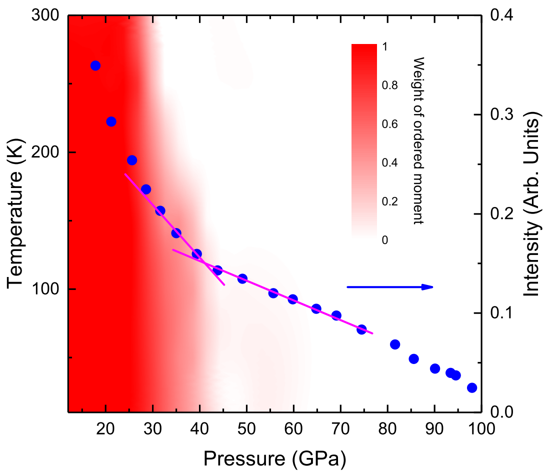

FIG. 5: (color online). The magnetic phase diagram of ε'-FeH. The weight of ordered moments shows two sharp changes around 26 and 43 GPa, which are related to the two magnetic phase transitions. The deduced difference intensity from the x-ray emission spectroscopy measurements also shows anomaly around 43 GPa, which indicates that the local magnetic moments are changed in the course of the magnetic phase transition.

also, references[22,23]therein). The derived portion of the satellite intensity should proportional to the total local magnetic moment in the material.

Unlike the magnetic transition from the α-iron to the ε-Fe, when the magnetic moment decreases to zero[24], the integrated difference of normalized spectra of ε'-FeH does not show any significant anomaly around 26 GPa, which indicates that the local magnetic moment is not quenched at the first magnetic transition. Around second magnetic transition, the XES shows anomaly, which indicates that the local magnetic moment changes sharply at the second magnetic transition. Below 43 GPa, the local magnetic moment decreases rapidly with increasing pressure, however, it still has some remaining value at higher pressure and may be even sustained above 100 GPa.

Our results indicate that the magnetic phase diagram in ε'-FeH is much more complex than previously thought. There are at least two magnetic phase transitions at high pressure due to the two inequivalent iron sites. The first magnetic transition is related to the loss of the ferromagnetism at the Fe2 site and slight decrease of the hyperfine field at the Fe1 site. The second magnetic transition above 43 GPa is related to the loss of magnetic order at the Fe1 site. The remaining small portion of ordered magnetic moments at higher pressure may be related to the disorder in the sample, e. g. due to the presence of stacking faults in the dhcp iron lattice[20]. The discovery of the two magnetic transitions is consistent with the anomalous compression behavior in the range from 30 to 50 GPa[14]. The second magnetic transition explains also the change of the sound velocity slope above 40 GPa in the previous inelastic nuclear resonance x-ray scattering study[12]. From the XES experiment, the local magnetic moment is gradually suppressed with increasing pressure. However, unlike the sudden loss of local moments in the compressed Fe, the ε'-FeH still has remaining local magnetic moment above 43 GPa, although the magnetic ordering is almost suppressed at these pressures. Our results clearly indicate that the ε'-FeH sustains magnetic ordering and the local magnetic moments in a much broader pressure range than previously expected. Such behavior maybe strongly correlated with its particular crystal structure. As we know, the cores of many planets and satellite bodies contain large quantities of iron, including Earth and Moon. The satellites of Jupiter and Saturn also contain large amounts of water, which could be a source of hydrogen for formation of iron hydride. Since hydrogen is the most abundant element in the Universe, ε'-FeH may form in interiors of many planetary bodies in our Solar system and across the Universe. Our results of the unexpected magnetic properties of ε'-FeH may have important implication to understanding the origins and variation of the magnetic fields and magnetic anomalies in the planetary bodies having no liquid core to sustain the magnetic dynamo effects. Since we expect that the major form of Fe in gas and icy giant planets is in various hydride phases, FeH may be present in massive eruptions during volcanic activity in the atmospheres of such planets, and may thus be responsible for some of the observed magnetic anomalies in such seismically active zones.

In conclusion, we have mapped out the detailed magnetic phase diagram of the ε'-FeH. Unexpectedly, we find two magnetic phase transitions. This behavior is due to the existence of the two inequivalent iron sites, which loose their magnetic ordering at different pressures. Our results account for the large difference in the predicted and observed magnetic collapse pressures between experiment and theoretical calculations. These results may have important implications for understanding of the magnetic and physical properties of planetary interiors and magnetic anomalies in gas and icy planets.

Acknowledgments

HPCAT operations are supported by DOE-NNSA under award no. DE-NA0001974 and DOE-BES under award no. DE-FG02-99ER45775, with partial instrumentation funding by NSF. APS is supported by DOE-BES, under contract no. DE-AC02-06CH11357. Sector 3 operations are partially supported by COMPRES, the Consortium for Materials Properties Research in Earth Sciences under NSF Coop-erative Agreement EAR-1606856. J. Y. acknowledges support by the CAS Pioneer Hundred Talents Program. VVS acknowledges support from the Thousand Talent Program by the State Council of the People's Republic of China.

* Electronic address: yingjj@ustc.edu.cn
† Electronic address: vstruzhkin@carnegiescience.edu

[1] F. Birch, J. Geophys. Res. **57**, 227-286 (1952).
[2] H.-K. Mao, Y. Wu, L. C. Chen, and J. F. Shu, J. Geophys. Res. **95**, 21737-21742 (1990).
[3] R. Jeanloz, Annu. Rev. Earth Planet. Sci. **18**, 357-387 (1990).
[4] Y. Fukai, Nature, **308**, 174-175 (1984).
[5] T. Suzuki, S. Akimoto, and Y. Fukai, Phys. Earth Planet. Inter. **36**, 135-144 (1984).
[6] Q. Williams, and R. J. Hemley, Annu. Rev. Earth Planet. Sci. **29**, 365-418 (2001).
[7] O. Mathon, F. Baudelet, J. P. Itié, A. Polian, M. d'Astuto, J. C. Chervin, and S. Pascarelli, Phys. Rev. Lett. **93**, 255503 (2004).
[8] K. Shimizu, T. Kimura, S. Furomoto, K. Takeda, K. Kontani, Y. Onuki, and K. Amaya, Nature **412**, 316-318 (2001).
[9] J. V. Badding, R. J. Hemley, and H. K. Mao, Science, **253**, 421-424 (1991).
[10] N. Ishimatsu, T. Shichijo, Y. Matsushima, H. Maruyama, Y. Matsuura, T. Tsumuraya, T. Shishidou, T. Oguchi, N. Kawamura, M. Mizumaki, T. Matsuoka, and K. Takemura, Phys. Rev. B **86**, 104430 (2012).
[11] T. Matsuoka, N. Hirao, Y. Ohishi, K. Shimizu, A. Machida, and K. Aoki, High Pressure Research **31**, 64-67 (2011).
[12] W. Mao, W.Sturhahn, D. Heinz, H. Mao, J. Shu, and R. Hemley, Geophys. Res. Lett. **31**, L15618 (2004).
[13] C. Elsässer, J. Zhu, S. G. Louie, B. Meyer, M. Fähnle, and C. T. Chan, J. Phys.: Condens. Matter **10**, 5113-5129 (1998).
[14] N. Hirao, T. Kondo, E. Ohtani, K. Takemura, and T. Kikegawa, Geophys. Res. Lett. **31**, L06616 (2004).
[15] A. G. Gavriliuk, A. A. Mironovich, and V. V. Struzhkin, Rev. Sci. Instrum. **80**, 043906 (2009).
[16] J.Y. Zhao, W. Bi, S. Sinogeikin, M.Y. Hu, E.E. Alp, X.C. Wang, C.Q. Jin, and J.F. Lin, Rev. Sci. Instrum. **88**, 125109 (2017).
[17] W. Bi, J. Zhao, J. Lin, Q. Jia, M.Y. Hu, C. Jin, R. Ferry, W. Yang, V. Struzhkin, and E.E. Alp, J. Synchrotron Radiat. **22**, 760 (2015).
[18] W. Sturhahn, Hyperfine Interactions **125**, 149-172 (2000).
[19] G. Schneider, M. Baier, R. Wordel, F. E. Wagner, V. E. Antonov, E. G. Ponyatovsky, Yu. Kopilovskii, and E. Makarov, J. Less-Common Met. **172-174**, 333-42 (1991).
[20] V. E. Antonov, M. Baier, B. Dorner, V. K. Fedotov, G. Grosse, A. I. Kolesnikov, E. G. Ponyatovsky, G. Schneider, and F. E. Wagner, J. Phys.: Condens. Matter **14**, 6427-6445 (2002).
[21] See Supplemental Material at [URL will be inserted by the production group] for details of analysing the XES spectra.
[22] G. Vankó, T. Neisius, G. Molnár, F. Renz, S. Kárpáti, A. Shukla, and F. M. F. de Groot, The Journal of Physical Chemistry B **110**, 11647 (2006).
[23] J. Ying, H. Lei, C. Petrovic, Y. Xiao, and V. V. Struzhkin, Phys. Rev. B **95**, 241109 (2017).
[24] J. P. Rueff, M. Krisch, Y. Q. Cai, A. Kaprolat, M. Hanfland, M. Lorenzen, C. Masciovecchio, R. Verbeni, and F. Sette, Phys. Rev. B **60**, 14510 (1999).